Journal of Veterinary Science

JVS

Original Article
Microbiology

Check for updates

Transcriptome sequencing revealed the inhibitory mechanism of ketoconazole on clinical *Microsporum canis*

Mingyang Wang [ID] [1,†], **Yan Zhao** [ID] [1,†], **Lingfang Cao** [ID] [1], **Silong Luo** [ID] [1], **Binyan Ni** [ID] [2], **Yi Zhang** [ID] [1,*], **Zeliang Chen** [ID] [1,*]

[1]Key Laboratory of Livestock Infectious Diseases in Northeast China, Ministry of Education, College of Animal Science and Veterinary Medicine, Shenyang Agricultural University, Shenyang 110866, China
[2]Qingdao Vetlab Biotechnology Co., Ltd., Qingdao 266109, China

OPEN ACCESS

ABSTRACT

Background: *Microsporum canis* is a zoonotic disease that can cause dermatophytosis in animals and humans.

Objectives: In clinical practice, ketoconazole (KTZ) and other imidazole drugs are commonly used to treat *M. canis* infection, but its molecular mechanism is not completely understood. The antifungal mechanism of KTZ needs to be studied in detail.

Methods: In this study, one strain of fungi was isolated from a canine suffering with clinical dermatosis and confirmed as *M. canis* by morphological observation and sequencing analysis. The clinically isolated *M. canis* was treated with KTZ and transcriptome sequencing was performed to identify differentially expressed genes in *M. canis* exposed to KTZ compared with those unexposed thereto.

Results: At half-inhibitory concentration (½MIC), compared with the control group, 453 genes were significantly up-regulated and 326 genes were significantly down-regulated ($p < 0.05$). Quantitative reverse transcription polymerase chain reaction analysis verified the transcriptome results of RNA sequencing. Gene ontology enrichment analysis and Kyoto Encyclopedia of Genes and Genomes enrichment analysis revealed that the 3 pathways of RNA polymerase, steroid biosynthesis, and ribosome biogenesis in eukaryotes are closely related to the antifungal mechanism of KTZ.

Conclusions: The results indicated that KTZ may change cell membrane permeability, destroy the cell wall, and inhibit mitosis and transcriptional regulation through CYP51, SQL, ERG6, ATM, ABCB1, SC, KER33, RPA1, and RNP genes in the 3 pathways. This study provides a new theoretical basis for the effective control of *M. canis* infection and the effect of KTZ on fungi.

Keywords: *Microsporum canis*; transcriptome; ketoconazole

INTRODUCTION

Microsporum canis is a ubiquitous protozoan pathogenic fungus [1,2]. *M. canis* mainly infects dogs, cats, and other animals, and then the animal infects humans [3]. Children and

Generated by xmlinkpress

ORCID iDs

Mingyang Wang
https://orcid.org/0000-0003-3496-3633
Yan Zhao
https://orcid.org/0000-0002-2169-2777
Lingfang Cao
https://orcid.org/0000-0002-7779-1918
Silong Luo
https://orcid.org/0000-0003-0424-1728
Binyan Ni
https://orcid.org/0000-0001-5066-9229
Yi Zhang
https://orcid.org/0000-0002-7854-1312
Zeliang Chen
https://orcid.org/0000-0003-4765-184X

Conflict of Interest

The authors declare no conflicts of interest.

Author Contributions

Conceptualization: Zhang Y, Wang M; Funding acquisition: Chen Z, Zhang Y; Methodology: Zhao Y, Cao L, Luo S; Project administration: Chen Z, Zhang Y; Validation: Zhao Y, Ni.B; Writing - original draft: Wang M; Writing - review & editing: Zhang Y.

immunocompromised individuals are more readily infected [4]. The main symptoms are hair loss, tinea capitis, tinea pedis, and onychomycosis [1,5]. Currently, various oral and topical antifungal drugs such as griseofulvin, terbinafine, itraconazole (IT), fluconazole (FLZ), and imidazole drugs are commonly used to control *M. canis* infection [6], among which ketoconazole (KTZ), as an imidazole drug, is the most frequently used [7]. Imidazoles are synthetic antifungal drugs that can selectively inhibit fungal cytochrome P-450-dependent 14-α-demethylase, change the permeability of cell membranes, causing the loss of important intracellular substances, leadingto fungal death [8]. Imidazole exhibits selective toxicity to fungi and this is mainly related to the inhibition of ergosterol biosynthesis and interference with other membrane lipids [9,10]. Although the antifungal mechanism of KTZ is similar to other imidazole drugs, its potential antifungal mechanism warrants further elucidation.

Through transcriptome sequencing technology, it is possible to obtain almost all transcript sequence information of a species in a certain state [11,12]. Transcriptome research allows the study of gene function and gene structure at a holistic level, revealing specific biological processes, and has been widely used in basic research, clinical diagnosis, and drug research and development [11-13]. In this study, we utilised transcriptome sequencing to explore differentially expressed genes (DEGs) and the pathways regulated by DEGs of *M. canis* after KTZ exposure, which clarified the underlying molecular mechanisms, signalling pathways of inhibition of KTZ on *M. canis*. Our study provides a new theoretical basis for the effective control of *M. canis* infection and the mechanism of KTZ inhibition on fungi.

MATERIALS AND METHODS

Cultivation and identification of *M. canis*

M. canis samples were taken from the skin of dogs suffering from skin diseases from an animal hospital in Shenyang, China. Subsequently, clinical samples were cultured using Sabouraud's Dextrose Agar medium (Coolaber, China), and colonies similar to the morphology of *M. canis* were isolated and purified by using potato dextrose agar (PDA) medium (Solarbio, China). Subsequently, Tryptone Soy Broth (Solarbio) was cultured in a fungus incubator at 28°C for 96 h, and the concentration of the fungal solution was adjusted to 2×10^4 CFU/mL. KTZ was purchased from Solarbio Ltd. (Solarbio) and dissolved in dimethyl sulfoxide (DMSO). The experiment was divided into 2 groups: the test group (T4,T5, and T6) treated with KTZ at a concentration of ½MIC for 6 h, and the control group (T1,T2, and T3) treated with DMSO at the same concentration. Tests on specimens in each group were repeated 3 times.

Identification of *M. canis*

The purified and cultured fungi were subjected to Diff-Quik® staining, morphological observation, and 18s ribosomal DNA (rDNA) sequence analysis. The DNA of *M. canis* was extracted using the Ezup column fungal genomic DNA extraction kit (Sangon Biotech Co., Ltd., China). Polymerase chain reaction (PCR) was carried out to amplify the DNA of *M. canis*. The primer sequences used for PCR were (NS1: f:5′-GTAGTCATATGCTTGTCTC-3′ and NS6: 5′-GCATCACAGACCTGTTATTGCCTC-3′). PCR was performed under following conditions: a hot start at 95°C for 4 min, then 30 cycles of 94°C (45 sec), 55°C (45 sec), and 72°C (60 sec), followed by extension at 72°C for 10 min. The resulting PCR amplification products were sequenced by Sangon Biotech Co., Ltd. BLAST (http://www.ncbi.nlm.nih.gov) was used to

identify sequences similar to the *M. canis* gene. All similar sequences were found from NCBI and a phylogenetic tree built after DNASTAR's alignment.

The minimum inhibitory concentration of KTZ against *M. canis*

M. canis and RPMI1640 medium were thoroughly mixed, centrifuged, and the fungal suspension obtained; the concentration of the RPMI1640 fungal suspension was adjusted to 4×10^4 CFU/mL. According to the CLSI M27-A standard, a drug susceptibility test was carried out on *M. canis* by micro-broth dilution method. We inoculated the fungal solution into a 96-well plate, dissolved KTZ with DMSO and added it to the fungal solution so that the final concentration of KTZ therein was 0 μg/mL, 0.195 μg /mL, 0.39 μg/mL, 0.78 μg/mL, 1.56 μg/mL, 3.13 μg/mL, 6.25 μg/mL, 12.5 μg/mL, and 25 μg/mL. The same concentration of DMSO without KTZ was used as a negative control. The 96-well plate was placed in an incubator and held at 28℃ for 7 days whereafter the optical density value was measured.

Library preparation for RNA and transcriptome sequencing

Total RNA was isolated from samples using the TRUEscript RT MasterMix (XinBaiJi Biotech, China) according to manufacturer's instructions. According to the manufacturer's instructions, NanoDrop 2000 (Thermo Fisher Scientific, USA) was used to measure the RNA concentration and purity, and the Agilent Bioanalyzer 2100 system (Agilent Technologies, USA) was employed to identify RNA integrity.

After the total RNA passed quality inspection, the magnetic beads connected to Oligo (dT) were used to enrich the eukaryotic messenger RNA (mRNA). The extracted mRNA was randomly interrupted into short fragments by RNA fragmentation buffer. Using fragmented mRNA as a template, a single-stranded complementary DNA (cDNA) was synthesised using random hexamers with 6 bases. Then buffer, dNTPs, RNaseH, and DNA polymerase I (Pol I) were added for double-strand cDNA synthesis. AMPure XP beads were used to purify double-stranded products, and the activities of T4 DNA polymerase and Klenow DNA polymerase were used to repair the sticky ends of DNA to form blunt ends. AMPureXP beads were used to perform fragment selection. Finally, PCR amplification was performed to obtain the final sequencing library. After the library was qualified, the Illumina Hiseq4000 was used for sequencing.

Data analysis

Cutadapt and internal Perl scripts were utilised to delete reads that contain adapter contamination and low-quality or uncertain bases. FastQC (www.bioinformatics. babraham.ac.uk/projects/fastqc/) was used to identify the quality of the sequence, including determining the quality scores Q20 and Q30 and the GC content of the clean data. All downstream analyses used high-quality clean data. Then we compared the high-quality sequence obtained after quality control with the designated reference genome.

Differential expression analysis

Differential expression analyses of 2 groups were performed using the DESeq2. The resulting *p* values were adjusted using the Benjamini and Hochberg's approach for controlling the false discovery rate. Genes with an adjusted *p* value of less than 0.01 found by DESeq2 were assigned as differentially expressed.

Gene ontology (GO) and KEGG pathway enrichment analyses

GO and KEGG databases were used for enrichment analysis of DEGs to ascertain the functions of DEGs. The Goseq R software package was used for the GO enrichment analysis

of DEGs. KOBAS software was employed to test the statistical enrichment of DEGs in the KEGG pathway.

Verification of DEGs

Total RNA was isolated from samples using TRUEscript RT MasterMix (XINBAIJI Biotech) according to manufacturer's instructions. The A260/A280 ratio of RNA was detected using an ultra-micro-nucleic acid protein analyser (Analytik Jena AG, Germany). When the A260/A280 ratio of RNA ranged from 1.8 to 2.0, it was used in subsequent experiments.

According to the instructions provided by the manufacturer, the first strand of cDNA was synthesised using TransScript First-Strand cDNA Synthesis kit (AiDLAB Biotech, China). Thereafter, according to the manufacturer's requirements, quantitative reverse transcription PCR (qRT-PCR) was conducted on an ABI 7500 real-time PCR system using SYBR Green QPCR Mix (DF Biotech, China) under the following conditions: thermal cycling denaturation at 95℃ for 3 min, followed by 40 cycles at 95℃ for 10 sec, annealing at 60℃ for 30 sec, and then extension. PheRS can be used as an internal reference gene. Finally, the relative change in mRNA was calculated using the $2^{-\Delta\Delta Ct}$ method. **Table 1** displays the primers used in the experiment. The primers were synthesised by Sangon Biotech Co., Ltd.

Statistical analysis

All statistical tests were conducted using SPSS 19.0 software (IBM, USA) and the results were expressed as mean ± standard deviation ($X \pm$ SD). To reveal the difference between 2 groups, 2-tailed Student's *t*-tests were used and significant differences among multiple groups were evaluated by using 1-way analysis of variance and least significant difference methods. Differences of $p < 0.05$ were considered significant.

Table 1. Primer sequences of messenger RNA used for quantitative real-time polymerase chain reaction

Gene name	Primer sequence (5'-3')	Annealing temperature (℃)
SC	F: ACTGTTGGTGATGGATAC	58
	R: ACTTGGTTAGAGACTTTGT	
CYP51	F: AGATATGGTGTGGAACTTA	58
	R: CATCAATAGAGCAATCATCAT	
SQLE	F: ATTTCCCGCCCATACTTA	58
	R: AACTGATGCTGAAGGTAGA	
ERG6	F: TGAACAACTACTATGACCTT	58
	R: GTGATTGCCTGAAGAAAG	
ABCB1	F: CAGCAGTGACGCCTTATC	58
	R: ATAGAGTATGAAGTTGGAGTGATG	
RPA1	F: ATTGCCAACTTGCTTCTC	58
	R: CGTAAGATGCCGATAGACT	
ATM	F: CTCAATGGTCTGCGGAAT	58
	R: AGGCTGTGGTAGTAATGGT	
RNP	F: GATTGTCGTGGAGAAACTTA	58
	R: TGCCGATTCATTGGTAAC	
KRE33	F: CTATACCATCCTCCAGTCAA	58
	R: TGCCTATGTTGCCTATGA	
PheRS	F: CTTGAGCCGAGAACTACT	58
	R: GGTCTCGTTCGTTATCGCAATT	

RESULTS

Identification of *M. canis*

The isolated *M. canis* colony was white, the mycelium on the PDA medium appeared in the form of white wool, and the colony exuded a yellow pigmented secretion (**Fig. 1A**). After Diff-Quik staining, the fungus was found to be fusiform, thick, rough, thorny, and able to produce large conidia (**Fig. 1B**). The DNA sequencing results showed that the 18s rDNA sequence of the isolated fungal strain was highly homologous to the 18s rDNA sequence of the *M. canis*. A phylogenetic tree was constructed with similar 18s rDNA sequences (**Fig. 2**). The results indicated that the isolated fungal strain is closely related to *M. canis* area under the first moment curve. According to the phylogenetic analysis of the morphology and 18s rDNA sequence, the fungal strain was identified as *M. canis*.

Determination of MIC of KTZ

As shown in **Fig. 3**, KTZ plays a significantly inhibitory role in the growth of *M. canis*. The results showed that the MIC of KTZ against *M. canis* was 1.56 µg/mL.
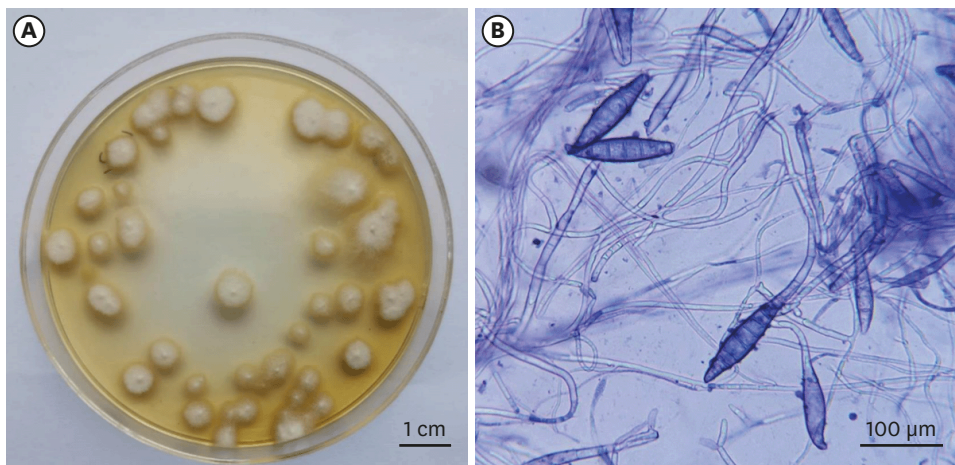

Fig. 1. Morphological characteristics of *M. canis*. (A) Colonies of *M. canis* strain on potato dextrose agar plates. (B) Diff-Quik staining of *M. canis* (10 × 40).
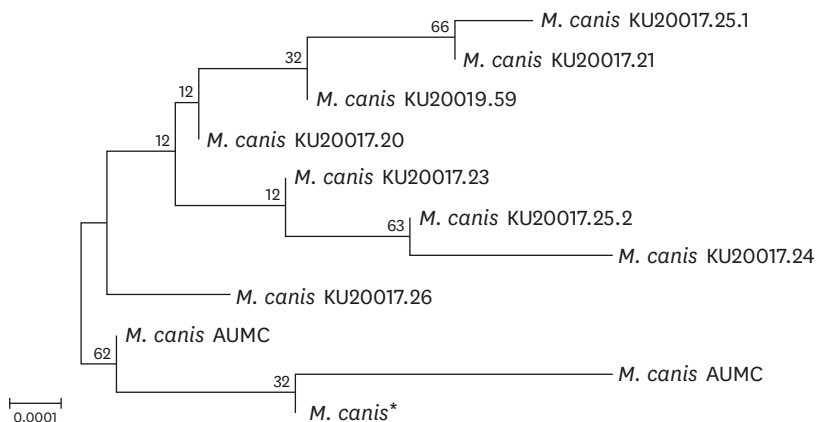

Fig. 2. Homology analysis based on partial 18s ribosomal DNA sequences of the *M. canis* and the related microorganisms.
AUMC, area under the first moment curve.
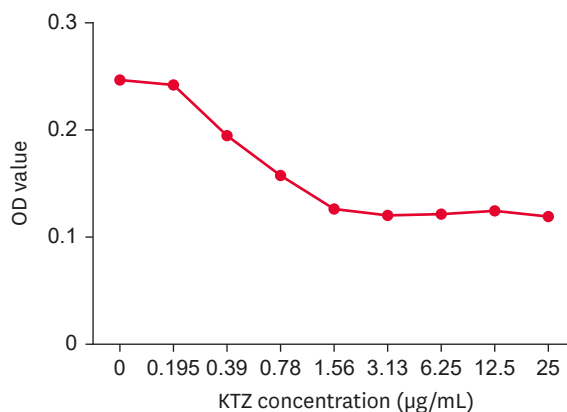*The DNA sequence of *M. canis* compared here.

Fig. 3. Rate of inhibition of *M. canis* at different concentrations.
OD, optical density; KTZ, ketoconazole.

Statistics pertaining to DEGs

As shown in the volcano diagram of DEGs in **Fig. 4**, there are 779 DEGs, of which 453 DEGs are up-regulated and 326 DEGs are down-regulated.

DEGs performed cluster analysis and cluster genes had the same or similar expression patterns. The clustering results of DEGs are shown in **Fig. 5**. The expression levels of DEGs in the same group were similar. The expression levels of DEGs in different groups differed. The results show that the sample repeatability was good, and that KTZ significantly changed the gene expression of *M. canis*.
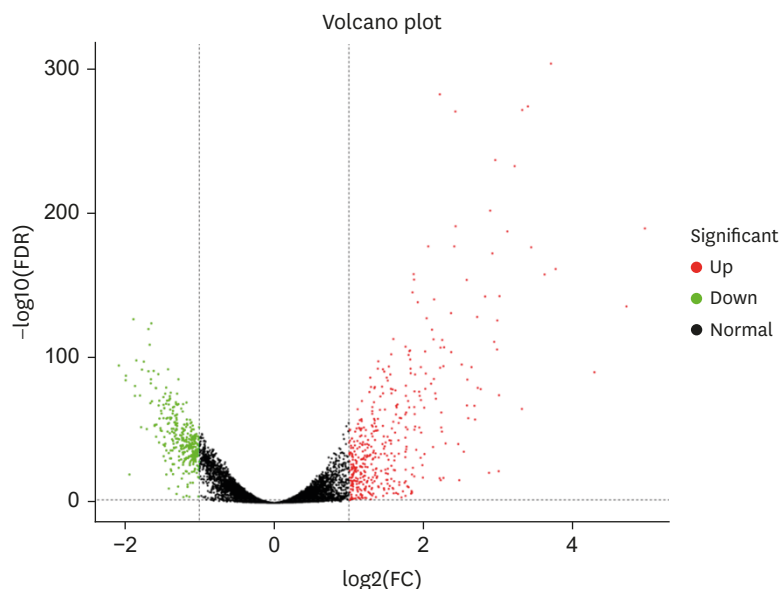

Fig. 4. Differential gene expression volcano diagram. Each point in the differential gene expression volcano diagram represents a gene, and the abscissa represents the logarithmic value of the difference in the expression of a certain gene of the 2 samples; the ordinate refers to the negative logarithm of the statistically significant change in gene expression. In the figure, green dots represent down-regulated DEGs, red dots are up-regulated DEGs, and black dots represent non-DEGs.
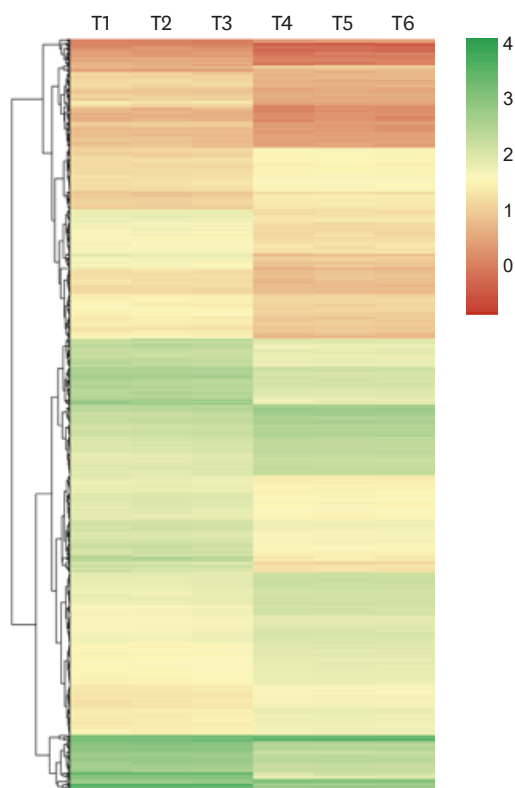DEG, differentially expressed gene.

Fig. 5. Cluster analysis of DEGs. The abscissa represents the sample name and the clustering result of the sample, and the ordinate represents the clustering result of the DEGs. The different columns in the figure represent different samples, where control samples are T1, T2, and T3, and ketoconazole samples are T4, T5, and T6. Different rows represent different genes. The color represents $\log_{10}$ (FPKM + 0.000001) of gene expression in the sample. DEG, differentially expressed gene.

GO enrichment analysis

Through GO annotation, 779 DEGs were enriched and analysed from 3 perspectives: biological process, cell composition, and molecular function (**Fig. 6**).

In the "biological process" category, the subcategories of "biological process" and "cellular process" have the most enriched DEGs. In the category of "cell components", "cells", "cell parts", "organelles", and "membrane parts" have the most enriched DEGs. In the category of "molecular function", the 2 most enriched subcategories of DEGs are "binding" and "catalytic activity".

KEGG annotation and pathway enrichment analysis

As shown in **Fig. 7**, DEGs are highly enriched in the 3 pathways of RNA polymerase, steroid biosynthesis, and ribosome biogenesis in eukaryotes. Therefore, these 3 pathways were selected for follow-up research.

qRT-PCR identification of DEGs

Ten DEGs, including SC, CYP51, SQLE, ERG6, ABCB1, RPA1, ATM, RNP and KRE33, were screened from 3 pathways of RNA polymerase, steroid biosynthesis, and ribosome biogenesis in eukaryotes (**Table 2**). The expression levels of DEGs were identified by qRT-PCR. As shown in **Fig. 8**, DEGs SC, CYP51, SQLE, ERG6, and ABCB1 in the KTZ group were up-regulated ($p < 0.05$), and the expressions of RPA1, ATM, RNP and KRE33 were down-regulated compared
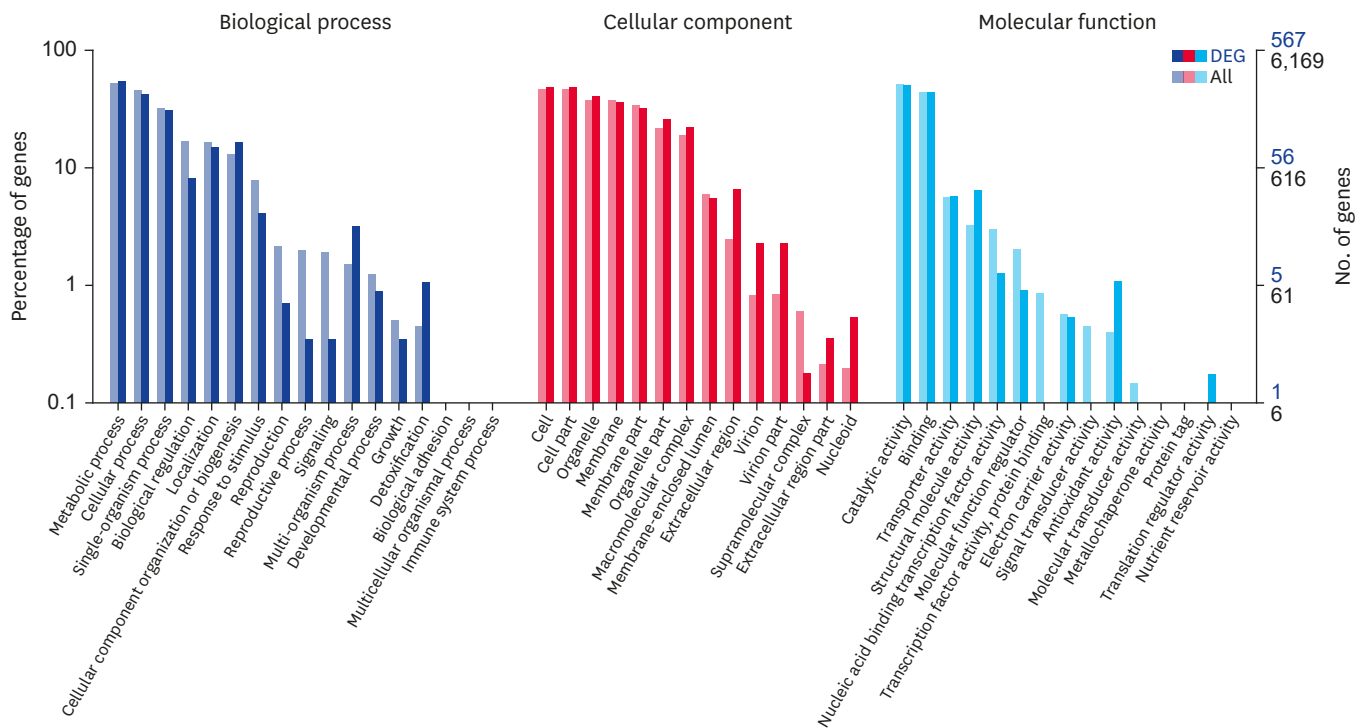
Fig. 6. GO enrichment analysis of DEGs. The abscissa is the GO classification, the left-hand ordinate is the percentage of the number of genes, that on the right is the number of genes.
GO, gene ontology; DEG, differentially expressed gene.

with the control group ($p < 0.05$). The experimental results of qRT-PCR were aligned with the results of transcriptome sequencing.

DISCUSSION

The antifungal mechanism of the most commonly used clinical imidazole drugs is very complex. In addition to inhibition of the activity of 14α-demethylase, some imidazole drugs also exert an inhibitory effect on other related enzymes present on the cell membrane [8,14]. For example, when *Candida albicans* is treated with voriconazole, an accumulation of yeast sterols and squalyl alcohol is found [8,15], however, it is unclear whether this result is ascribed to the interaction between voriconazole and some enzymes related to ergosterol synthesis on the cell membrane, or the secondary effect of 14α-demethylase activity after being inhibited. Besides, the mechanism of action of imidazole drugs is also related to the target, such as FLZ and IT, in addition to inhibiting the 14α-demethylase activity of *Cryptococcus neoformans*, it can also inhibit the reduction of obtusifolione to the corresponding obtusifoliol [16,17]. This effect causes the accumulation of methylated sterol precursors to affect the function of cell membranes [16,17], therefore, the antifungal mechanism of imidazole drugs requires further study. KTZ is commonly used in clinical practice to treat *M. canis* infections. To study the antifungal mechanism of KTZ on *M. canis*, we collected and purified a fungus from dogs with fungal skin diseases. After morphological observation and DNA sequence alignment, the fungus was identified as *M. canis*.
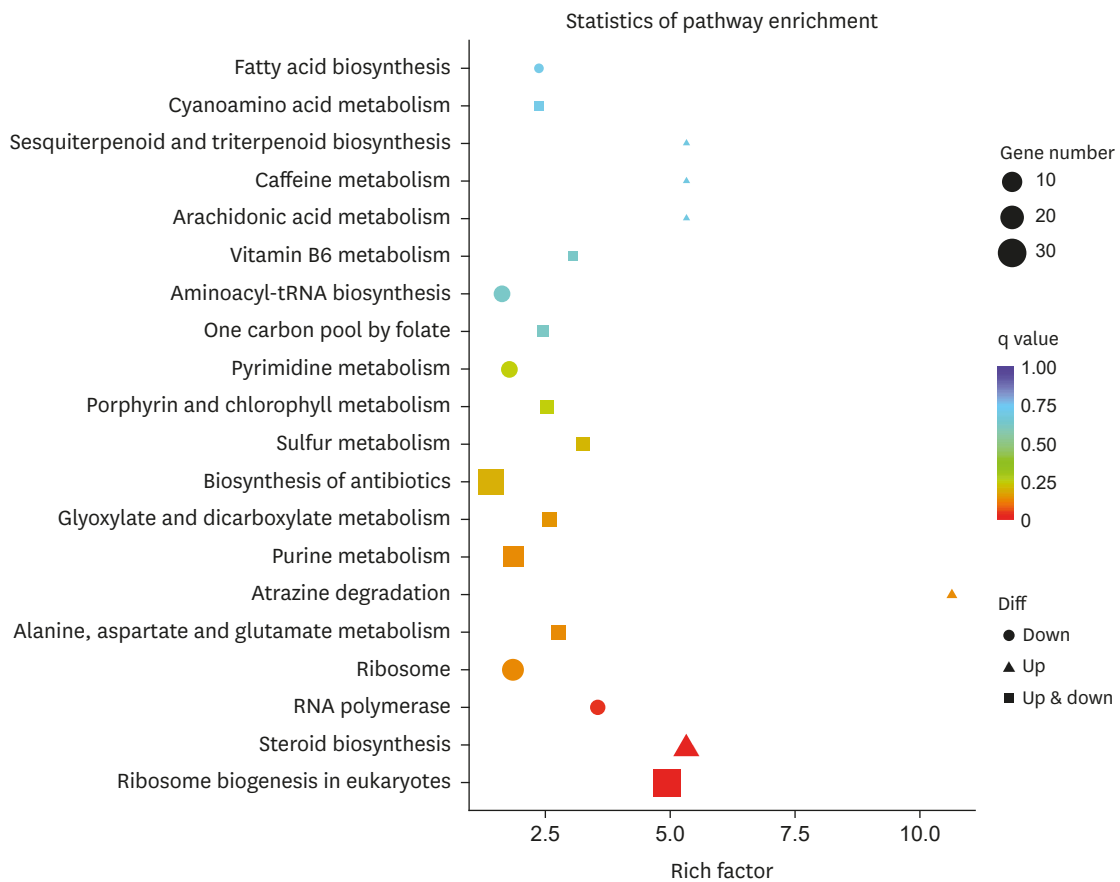
Fig. 7. Enriched scatter plot of KEGG pathway of differentially expressed genes. Each circle in the figure represents a KEGG channel. The abscissa represents the enrichment factor and the ordinate represents the name of the channel.
KEGG, Kyoto Encyclopedia of Genes and Genomes.

Table 2. Differentially expressed genes were screened from 3 pathways of RNA polymerase, steroid biosynthesis, and ribosome biogenesis in eukaryotes

Gene name	Gene ID	Fold change (up/down)
SC	Gene-MCYG_05458	Up
CYP51	Gene-MCYG_07307	Up
SQLE	Gene-MCYG_02365	Up
ERG6	Gene-MCYG_05366	Up
ABCB1	Gene-MCYG_06184	Up
RPA1	Gene-MCYG_00357	Down
ATM	Gene-MCYG_03240	Down
RNP	Gene-MCYG_02807	Down
KRE33	Gene-MCYG_05927	Down

Based on the experiments of Xiao et al. [18], we used a half MIC of KTZ to treat *M. canis*. This is a stress concentration for *M. canis* that can better reflect the antifungal mechanism of KTZ on *M. canis*. Sequencing results showed that after KTZ treatment, a total of 779 genes were significantly differentially expressed, of which 453 genes were up-regulated and 326 genes were down-regulated. These genes will be the key to explore the antifungal mechanism of KTZ on *M. canis*.

In the results of GO enrichment analysis, the DEGs were most abundant in "biological process", "cell process", "cell", "cell part", "organelle", "membrane part", "binding", and
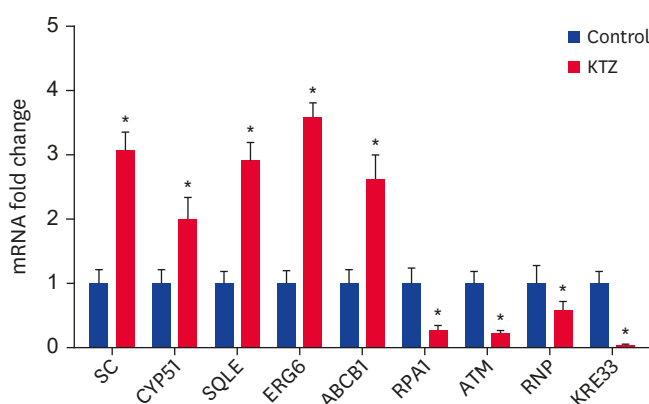
Fig. 8. Quantitative reverse transcription polymerase chain reaction analyses of the mRNA expression levels of SC, CYP51, SQLE, ERG6, ABCB1, RPA1, ATM, RNP, and KRE33 in the control and KTZ groups.
mRNA, messenger RNA; KTZ, ketoconazole.
*$p < 0.05$.

"catalytic activity" subcategories. Coincidentally, inhibition of fungal cytochrome P-450-dependent 14α-demethylase changes the permeability of the cell membrane, resulting in the loss of intracellular nutrients and organelles: this is the main antifungal mechanism of KTZ [8-10], therefore, we speculated that the antifungal mechanism of KTZ against *M. canis* was closely related to the presence of these differential genes.

The further to study the role of these differential genes in the antifungal mechanism of KTZ on *M. canis* we screened 3 pathways of RNA polymerase, steroid biosynthesis, and ribosome biogenesis in eukaryotes by KEGG enrichment analysis. The DEGs in these 3 pathways were verified by qRT-PCR. The results of qRT-PCR of the differential genes are consistent with the sequencing results, which show that our sequencing results were correct.

Among the DEGs, CYP51 (sterol 14α-demethylase) is the most conserved cytochrome P450 enzyme in the entire system [19]. In eukaryotes, the P450 enzyme is an enzyme necessary for sterol biosynthesis, and sterol is an essential component of the plasma membrane, which is essential for maintaining the function of fungal cell membranes [20,21]. CYP51 protein is also a target for azole drugs. It demethylates the 14-α position of lanosterol to form ergosterol to change the permeability and fluidity of the cell membrane [21,22]. The up-regulation of CYP51 expression in this experiment indicated that KTZ may play an antifungal role by mediating the P450 enzyme regulated by CYP51.

The other 2 genes related to the cell membrane are squalene monooxygenase (SQLE) and ERG6. The SQLE is a key flavin adenine dinucleotide-dependent enzyme in the biosynthesis pathway of ergosterol and cholesterol, and it is a drug used to inhibit the growth of pathogenic fungi or lower cholesterol levels in potential targets [23]. Zare et al. [24]. found that, after treating *C. albicans* with Te nanoparticles (NPs) (0.2 mg/mL), Te NPs can inhibit SQLE and lead to an increase in the level of SQLE gene expression. This is consistent with our experimental results. Therefore, we speculate that KTZ can inhibit SQLE, so that squalene accumulates to kill *M. canis*. The ERG6 gene encodes the S-adenosylmethionine-dependent sterol C-24 methyltransferase in the ergosterol biosynthetic pathway [25]. Studies have shown that when fungi are resistant to azole drugs, ERG3 and ERG6 may play a role in the biosynthetic pathway of ergosterol [26]. The expression of ERG6 was significantly up-regulated in this experiment, which may be related to the resistance of *M. canis* to KTZ. In

addition, the active efflux of ATP binding cassette (ABC) superfamily proteins is found to be an important mechanism for resistance among azole antifungal drugs [8]. Therefore, we also speculated that the 2 genes of the ABC, ATM and ABCB1, are also involved in the resistance mechanism of *M. canis* to KTZ.

KTZ also affected genes related to the cell wall of *M. canis*. Among differential genes, the expression of Chitinase (SC) gene was significantly up-regulated. SC is an enzyme that can cleave the β-(1,4) glycosidic bond of chitin in the cell wall [27]. Chitin is an important component of the fungal cell wall, and is essential for maintaining the structural integrity of the fungal cell wall and the growth and survival of the fungus [28,29]. Therefore, KTZ may damage the cell wall of *M. canis* by regulating SC.

KTZ not only inhibits those genes related to the cell membrane and cell wall of *M. anis*, but also affects the genes responsible for *M. canis* growth, reproduction and transcription regulation. KRE33 (NAT10) is an N-acetyltransferase and studies have shown that NAT10 may play an important role in cell division by promoting the reorganisation of nucleolus and middle body in the late mitosis and the stabilisation of microtubules [30]. RPA1 is an RNA polymerase, and RNA Pol I is a highly synthetic enzyme that can transcribe rDNA and regulate the growth of eukaryotic cells [31]. RNA polymerases I and III are responsible for most nuclear transcription in actively growing cells, and their activity affects the biosynthetic capacity of the cell [32]. Ribonucleoprotein (RNP) is a protein associated with RNA [33]. It can combine with mRNA and non-coding RNA to form an RNP complex. They can coordinate the production of function-related proteins, so that the activity and stability of many RNAs are regulated after transcription [33,34]. The differential expressions of these genes change significantly, so we speculated that KTZ can inhibit the mitosis of *M. canis* cells by down-regulating the expression of the KRE33 gene and mediating the transcriptional regulation of *M. canis* by regulating RPA1 and RNP.

Our results revealed the potential mechanism of KTZ treatment against *M. canis* through transcriptome sequencing; however, the more detailed aspects of these findings should be clarified in future studies of gene function, such as gene knock-out experiments, so as to better describe the genes selected in this study.

In conclusion, 779 DEGs were screened by transcriptome sequencing. Among them, 453 DEGs were up-regulated and 326 DEGs were down-regulated. The results of GO and KEGG enrichment analysis showed that KTZ could change cell membrane permeability, destroy the cell wall, affect drug resistance, and inhibit mitosis and transcriptional regulation by regulating CYP51, SQL, ERG6, ATM, ABCB1, SC, KER33, RPA1, and RNP in *M. canis*.

REFERENCES

1. Binder B, Lackner HK, Poessl BD, Propst E, Weger W, Smolle J, et al. Prevalence of tinea capitis in Southeastern Austria between 1985 and 2008: up-to-date picture of the current situation. Mycoses. 2011;54(3):243-247.
   PUBMED | **CROSSREF**
2. Bond R, Morris DO, Guillot J, Bensignor EJ, Robson D, Mason KV, et al. Biology, diagnosis and treatment of *Malassezia* dermatitis in dogs and cats: clinical consensus guidelines of the world association for veterinary dermatology. Vet Dermatol. 2020;31(1):75.
   PUBMED | **CROSSREF**

3. Yin B, Xiao Y, Ran Y, Kang D, Dai Y, Lama J. *Microsporum canis* infection in three familial cases with tinea capitis and tinea corporis. Mycopathologia. 2013;176(3-4):259-265.
PUBMED | CROSSREF

4. Anemüller W, Baumgartner S, Brasch J. Atypical *Microsporum canis* variant in an immunosuppressed child. J Dtsch Dermatol Ges. 2008;6(6):473-475.
PUBMED | CROSSREF

5. Ginter-Hanselmayer G, Weger W, Ilkit M, Smolle J. Epidemiology of tinea capitis in Europe: current state and changing patterns. Mycoses. 2007;50 Suppl 2:6-13.
PUBMED | CROSSREF

6. Verma SB. Emergence of recalcitrant dermatophytosis in India. Lancet Infect Dis. 2018;18(7):718-719.
PUBMED | CROSSREF

7. Aneke CI, Otranto D, Cafarchia C. Therapy and antifungal susceptibility profile of *Microsporum canis*. J Fungi (Basel). 2018;4(3):107.
PUBMED | CROSSREF

8. Ghannoum MA, Rice LB. Antifungal agents: mode of action, mechanisms of resistance, and correlation of these mechanisms with bacterial resistance. Clin Microbiol Rev. 1999;12(4):501-517.
PUBMED | CROSSREF

9. Vanden Bossche H. Biochemical targets for antifungal azole derivatives: hypothesis on the mode of action. Curr Top Med Mycol. 1985;1:313-351.
PUBMED | CROSSREF

10. Borgers M, Van den Bossche H, De Brabander M. The mechanism of action of the new antimycotic ketoconazole. Am J Med. 1983;74(1B):2-8.
PUBMED | CROSSREF

11. Wang Z, Gerstein M, Snyder M. RNA-Seq: a revolutionary tool for transcriptomics. Nat Rev Genet. 2009;10(1):57-63.
PUBMED | CROSSREF

12. Lockhart DJ, Winzeler EA. Genomics, gene expression and DNA arrays. Nature. 2000;405:827-836.
PUBMED | CROSSREF

13. Costa V, Angelini C, De Feis I, Ciccodicola A. Uncovering the complexity of transcriptomes with RNA-Seq. J Biomed Biotechnol. 2010;2010:853916.
PUBMED | CROSSREF

14. Sheehan DJ, Hitchcock CA, Sibley CM. Current and emerging azole antifungal agents. Clin Microbiol Rev. 1999;12(1):40-79.
PUBMED | CROSSREF

15. Sanati H, Belanger P, Fratti R, Ghannoum M. A new triazole, voriconazole (UK-109,496), blocks sterol biosynthesis in *Candida albicans* and *Candida krusei*. Antimicrob Agents Chemother. 1997;41(11):1249-6.
PUBMED | CROSSREF

16. Ghannoum MA, Spellberg BJ, Ibrahim AS, Ritchie JA, Currie B, Spitzer ED, et al. Sterol composition of *Cryptococcus neoformans* in the presence and absence of fluconazole. Antimicrob Agents Chemother. 1994;38(9):2029-2033.
PUBMED | CROSSREF

17. Vanden Bossche H, Marichal P, Le Jeune L, Coene MC, Gorrens J, Cools W. Effects of itraconazole on cytochrome P-450-dependent sterol 14 alpha-demethylation and reduction of 3-ketosteroids in *Cryptococcus neoformans*. Antimicrob Agents Chemother. 1993;37(10):2101-2105.
PUBMED | CROSSREF

18. Xiao CW, Ji QA, Wei Q, Liu Y, Pan LJ, Bao GL. Digital gene expression analysis of *Microsporum canis* exposed to berberine chloride. PLoS One. 2015;10(4):e0124265.
PUBMED | CROSSREF

19. Galani K, Nissan TA, Petfalski E, Tollervey D, Hurt E. Rea1, a dynein-related nuclear AAA-ATPase, is involved in late rRNA processing and nuclear export of 60 S subunits. J Biol Chem. 2004;279(53):55411-55418.
PUBMED | CROSSREF

20. Lepesheva GI, Waterman MR. Sterol 14alpha-demethylase cytochrome P450 (CYP51), a P450 in all biological kingdoms. Biochim Biophys Acta. 2007;1770(3):407-477.
PUBMED | CROSSREF

21. Lepesheva GI, Friggeri L, Waterman MR. CYP51 as drug targets for fungi and protozoan parasites: past, present and future. Parasitology. 2018;145(14):1820-1836.
PUBMED | CROSSREF

22. Zhang J, Li L, Lv Q, Yan L, Wang Y, Jiang Y. The fungal CYP51s: their functions, structures, related drug resistance, and inhibitors. Front Microbiol. 2019;10:691.
PUBMED | CROSSREF

23. Nowosielski M, Hoffmann M, Wyrwicz LS, Stepniak P, Plewczynski DM, Lazniewski M, et al. Detailed mechanism of squalene epoxidase inhibition by terbinafine. J Chem Inf Model. 2011;51(2):455-462.
    PUBMED | CROSSREF

24. Zare B, Sepehrizadeh Z, Faramarzi MA, Soltany-Rezaee-Rad M, Rezaie S, Shahverdi AR. Antifungal activity of biogenic tellurium nanoparticles against *Candida albicans* and its effects on squalene monooxygenase gene expression. Biotechnol Appl Biochem. 2014;61(4):395-400.
    PUBMED | CROSSREF

25. Konecna A, Toth Hervay N, Valachovic M, Gbelska Y. ERG6 gene deletion modifies *Kluyveromyces lactis* susceptibility to various growth inhibitors. Yeast. 2016;33(12):621-632.
    PUBMED | CROSSREF

26. Morio F, Pagniez F, Lacroix C, Miegeville M, Le Pape P. Amino acid substitutions in the *Candida albicans* sterol Δ5,6-desaturase (Erg3p) confer azole resistance: characterization of two novel mutants with impaired virulence. J Antimicrob Chemother. 2012;67(9):2131-2138.
    PUBMED | CROSSREF

27. Xiao CW, Ji QA, Wei Q, Liu Y, Bao GL. Antifungal activity of berberine hydrochloride and palmatine hydrochloride against *Microsporum canis* -induced dermatitis in rabbits and underlying mechanism. BMC Complement Altern Med. 2015;15(4):177.
    PUBMED | CROSSREF

28. Ruiz-Herrera J, San-Blas G. Chitin synthesis as target for antifungal drugs. Curr Drug Targets Infect Disord. 2003;3(1):77-91.
    PUBMED | CROSSREF

29. Yang J, Zhang KQ. Chitin synthesis and degradation in fungi: biology and enzymes. Adv Exp Med Biol. 2019;1142:153-167.
    PUBMED | CROSSREF

30. Shen Q, Zheng X, McNutt MA, Guang L, Sun Y, Wang J, et al. NAT10, a nucleolar protein, localizes to the midbody and regulates cytokinesis and acetylation of microtubules. Exp Cell Res. 2009;315(10):1653-1667.
    PUBMED | CROSSREF

31. Neyer S, Kunz M, Geiss C, Hantsche M, Hodirnau VV, Seybert A, et al. Structure of RNA polymerase I transcribing ribosomal DNA genes. Nature. 2016;540(7634):607-610.
    PUBMED | CROSSREF

32. Vannini A. A structural perspective on RNA polymerase I and RNA polymerase III transcription machineries. Biochim Biophys Acta. 2013;1829(3-4):258-264.
    PUBMED | CROSSREF

33. Hopper AK, Nostramo RT. tRNA Processing and subcellular trafficking proteins multitask in pathways for other RNAs. Front Genet. 2019;10:96.
    PUBMED | CROSSREF

34. Keene JD. Ribonucleoprotein infrastructure regulating the flow of genetic information between the genome and the proteome. Proc Natl Acad Sci U S A. 2001;98(13):7018-7024.
    PUBMED | CROSSREF